








Cite this: *Chem. Commun.*, 2024, 60, 7077

Received 9th April 2024,  
Accepted 10th June 2024

DOI: 10.1039/d4cc01634c

[rsc.li/chemcomm](http://rsc.li/chemcomm)

# Improving the direct air capture capacity of grafted amines *via* thermal treatment†

Melinda L. Jue, <sup>a</sup> Nathan C. Ellebracht, <sup>a</sup> Mathew J. Rasmussen, <sup>b</sup>  
Elwin Hunter-Sellers,<sup>a</sup> Maxwell A. T. Marple, <sup>a</sup> Matthew M. Yung<sup>b</sup> and  
Simon H. Pang <sup>\*a</sup>

This study investigates the effects of elevated temperature thermal treatments on the direct air capture of CO<sub>2</sub> by aminosilane-grafted SBA-15 silica sorbents. Exposing samples to high temperatures (200–250 °C compared to 80–120 °C) in an inert environment resulted in improved CO<sub>2</sub> capacity (5–21%) that was sustained over multiple adsorption/desorption cycles.

Solely reducing the amount of carbon dioxide (CO<sub>2</sub>) produced is no longer a feasible strategy to mitigate the major effects of climate change due to the difficulty in decarbonizing certain sectors such as heavy industry and aviation.<sup>1</sup> To reach net-zero greenhouse gas emissions, carbon dioxide removal technologies, such as directly removing CO<sub>2</sub> from the atmosphere, are required.<sup>2</sup> This technology benefits from additional flexibility in partitioning the CO<sub>2</sub> capture process from the generation source and the ability to collocate the separations with energy generation or sequestration sites.<sup>3–5</sup>

Many classes of materials exhibit the ability to capture CO<sub>2</sub> from dilute feed streams, including zeolites, ion-exchange resins, and oxide minerals.<sup>6–10</sup> Solid CO<sub>2</sub> adsorbents for direct air capture (DAC) are typically operated in a cyclic adsorption–desorption process *via* temperature–vacuum swing desorption. Covalently grafted amine and supported oligo- and polyamine adsorbent materials have been studied extensively for their ability to reversibly chemisorb CO<sub>2</sub> with fast kinetics at low partial pressures of CO<sub>2</sub> and with relatively low temperature swings.<sup>5,11</sup> Typically, regeneration conditions around 80–120 °C are sufficient to remove bound CO<sub>2</sub> in adsorption processes, and rapid cycling is critical to the technoeconomic feasibility of amine-based DAC processes.<sup>12</sup> Higher regeneration temperature could potentially allow for more rapid and complete

desorption of CO<sub>2</sub>, minimizing the time that the sorbent spends in regeneration and increasing cyclic working capacity. However, repeated exposure to higher desorption temperatures may lead to sorbent degradation and increased energy consumption.<sup>11,13,14</sup>

In this work, we focus on aminosilanes covalently grafted onto porous oxide supports for use as DAC CO<sub>2</sub> sorbents, primarily (2-aminoethyl)-3-aminopropyltrimethoxysilane (designated ethyl diamine) grafted onto SBA-15 silica. This model system allows us to investigate amine-based adsorption fundamentals, despite the relatively low total amine content compared to aminopolymer-based DAC sorbents. Moreover, due to the covalent linkage between the amine and the support surface, grafted amines are not easily evaporated at high temperature, which can happen to smaller fragments of physically impregnated aminopolymers.<sup>15</sup> Here, we focus on three materials with varied grafting densities of the ethyl diamine (designated low, medium, and high, Table 1 and Table S1, ESI<sup>†</sup>). To assess the limits of thermal stability for grafted aminosilane-based sorbents, we investigated the effects of elevated temperature treatments on material performance and chemistry consisting of 12 hour holds at either 200, 250, or 300 °C in a N<sub>2</sub> atmosphere. N<sub>2</sub> was chosen to avoid any potential degradation from O<sub>2</sub> or CO<sub>2</sub> at elevated temperatures.<sup>13</sup> The elemental analysis results show a consistent loss in organic loading and an increase in the C/N ratio with increasing thermal treatment temperature, indicative of thermal cleavage of the grafted aminosilanes.<sup>16</sup>

The CO<sub>2</sub> capacity of the sorbents was determined using a thermogravimetric analyzer coupled with a mass spectrometer at the outlet (TGA-MS). The mass change due to CO<sub>2</sub> adsorption at 30 °C from a dry 410 ppm CO<sub>2</sub> in N<sub>2</sub> feed was measured with the TGA (Fig. S1–S3 and Table S2, ESI<sup>†</sup>). Fig. 1 shows the CO<sub>2</sub> capacity for each of the three samples before and after exposure to each thermal treatment temperature. Notably, the pseudo-equilibrium (12 hour) CO<sub>2</sub> capacity increased 5–21% when thermally treated between 200–250 °C, but significantly decreased when treated at 300 °C. These trends with temperature are also reflected in the uptake rate during the adsorption step (Fig. 1b). For the medium and high loading sorbents, the uptake rate is

<sup>a</sup> Materials Science Division, Lawrence Livermore National Laboratory, Livermore, CA 94550, USA. E-mail: pang6@llnl.gov

<sup>b</sup> Catalytic Carbon Transformation and Scale-up Center,

*National Renewable Energy Laboratory, Golden, CO 80401, USA*

† Electronic supplementary information (ESI) available: Materials, synthesis procedure, physisorption, elemental analysis, thermogravimetric analysis, DRIFTS, solid state NMR. See DOI: <https://doi.org/10.1039/d4cc01634c>

**Table 1** Combustion elemental analysis results for low, medium, and high loading ethyl diamine grafted SBA-15. The thermal treatments were conducted in N<sub>2</sub> for 12 hours. The C, H, and N content are the averages of duplicate measurements taken from the same sample

Samples	Amine loading (mol N kg <sup>-1</sup> )	Thermal treatment temperature (°C)	C (wt%)	H (wt%)	N (wt%)	C/N molar ratio
Low	2.38	—	7.78	1.71	3.34	2.33
	2.37	200	7.72	1.83	3.32	2.33
	2.26	250	7.67	1.77	3.16	2.43
	1.90	300	7.38	1.64	2.66	2.77
Medium	3.20	—	10.32	2.22	4.49	2.30
	3.22	200	10.33	2.41	4.52	2.29
	3.14	250	10.50	2.30	4.40	2.39
	2.64	300	9.94	2.11	3.70	2.69
High	3.78	—	12.06	2.67	5.30	2.28
	3.73	200	12.10	2.66	5.23	2.31
	3.62	250	12.00	2.73	5.08	2.36
	3.31	300	11.68	2.57	4.63	2.52

largely the same for the untreated, 200, and 250 °C treated samples. Once treated at 300 °C, the total capacity and uptake rate appreciably decrease due to the onset of thermal degradation of the aminosilanes.

The low loading ethyl diamine sample exhibited distinct uptake rate curves with each thermal treatment and generally the largest changes in CO<sub>2</sub> capacity both positively (200 °C) and negatively (300 °C), while the high loading samples were the least affected. In addition, the C/N ratio after 300 °C treatment from the elemental analysis reflects a 19% increase for the low loading sample, yet only a 10% increase for the high loading sample. This indicates that the lower loading samples are more susceptible to the changes induced by the thermal treatments. Higher grafting density may offer greater thermal cleavage

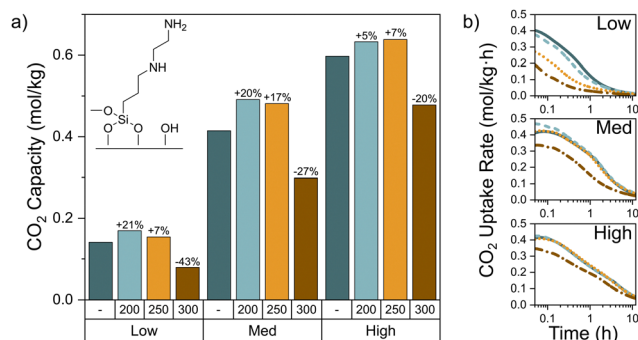


**Fig. 1** (a) The pseudo-equilibrium direct air capture (30 °C, 12 hours, 410 ppm CO<sub>2</sub> in N<sub>2</sub>) uptake capacity for SBA-15 sorbents grafted with low, medium, and high loadings of ethyl diamine. Each sample was exposed to either 200, 250, or 300 °C thermal treatment in N<sub>2</sub> for 12 hours prior to CO<sub>2</sub> uptake and compared against an untreated sample. The percentage change in capacity relative to the untreated sample is shown above each column. The chemical structure of ethyl diamine silane grafted to the surface of SBA-15 is shown in the upper left corner. (b) The instantaneous CO<sub>2</sub> uptake rate over the course of the adsorption step for the low (top), medium (middle), and high (bottom) loading samples. The colors represent the different thermal treatments, dark blue, solid – untreated; light blue, dashed – 200 °C; orange, dotted – 250 °C; and brown, dash-dotted – 300 °C.

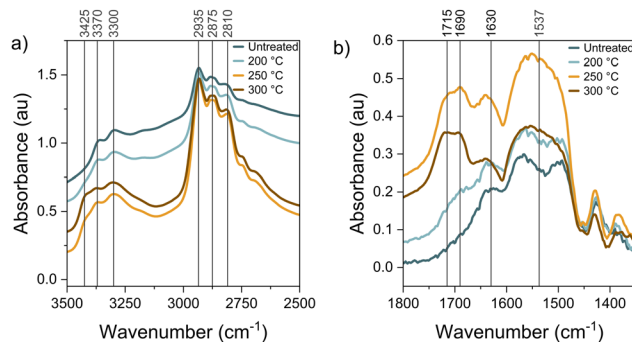


**Fig. 2** (a) The DRIFTS CH<sub>x</sub>/NH<sub>x</sub> stretching region for the high loading ethyl diamine grafted SBA-15 sorbent, untreated and exposed to thermal treatments (separate samples). Spectra measured in a N<sub>2</sub> environment. (b) DRIFTS CO<sub>2</sub> binding spectra for high loading ethyl diamine grafted SBA-15 sorbents untreated and exposed to thermal treatments. Spectra measured in a 1% CO<sub>2</sub>/He environment have the baseline spectra measured in a N<sub>2</sub> environment subtracted from them.

resistance by providing more possible hydrogen bonding sites for the grafted aminosilanes. In the absence of water, primary and secondary amines can theoretically bind CO<sub>2</sub> from air in a 2:1 N:CO<sub>2</sub> stoichiometry (amine efficiency = 0.5); at lower aminosilane grafting densities, these pairwise binding interactions are less common due to decreased silane proximity and as the stoichiometry shifts further below 2:1.<sup>17,18</sup> Changes to the surface functionality or loss of amine moieties due to thermal treatment would tend to have an outsized effect on low grafting density materials, as reflected in the trends found here.

To understand the surface behavior, we utilized diffuse reflectance infrared Fourier transform spectroscopy (DRIFTS) to probe the high loading ethyl diamine grafted SBA-15 samples during thermal treatment and CO<sub>2</sub> adsorption (Fig. S8, S9 and Tables S3–S5, ESI†). Fig. 2a highlights the CH<sub>x</sub> (2700–3000 cm<sup>-1</sup>) and NH<sub>x</sub> (3200–3400 cm<sup>-1</sup>) stretching regions of the samples in a dry inert atmosphere. The bands at 2810 and 2875 cm<sup>-1</sup> correspond to the symmetric C–H stretching modes while the band at 2935 cm<sup>-1</sup> corresponds to the asymmetric C–H stretching mode.<sup>19–21</sup> The N–H symmetric and asymmetric stretching bands are observed at 3300 and 3370 cm<sup>-1</sup>, respectively.<sup>22</sup> The relative intensities of the CH<sub>x</sub> bands compared to the NH<sub>x</sub> bands increase with increasing thermal treatment temperature, in agreement with the increase in C/N ratio from elemental analysis and <sup>13</sup>C NMR (Fig. S10, ESI†), suggesting that more amine moieties are cleaved from the alkyl linkers with increasing temperature.

Fig. 2b shows the CO<sub>2</sub> binding spectra for sorbents before and after thermal treatments. Thermal treatment at 200 °C has minimal effect on the CO<sub>2</sub> binding bands and agrees with the minor changes seen in the CH<sub>x</sub> and NH<sub>x</sub> stretching bands and small increase in the CO<sub>2</sub> capacity. The largest changes are seen after 250 °C thermal treatment, with increases to the bands centered around 1537 and 1630 cm<sup>-1</sup>, corresponding to the asymmetric vibration from the ammonium ion, and the bands near 1690 and 1715 cm<sup>-1</sup>, corresponding to carbamic acid stretching modes.<sup>22–24</sup> These changes in the CO<sub>2</sub> binding peak



intensities after thermal treatment indicate a shift towards the formation of carbamic acid.<sup>23</sup> Furthermore, the emergence of the O–H stretching vibration band with increasing temperature at 3425 cm<sup>−1</sup> (Fig. 2a) and <sup>13</sup>C–<sup>1</sup>H correlation measurements (Fig. S11 and S12, ESI†) may be attributed to an increase in hydrogen-bonded silanol groups that could result from several thermally-induced chemical changes. The hydrogen-bonded silanol and isolated silanol densities of silica have been shown to change from thermal treatments between 200–400 °C.<sup>25</sup> There is likely additional hydroxyl liberation from breaking the hydrogen bonding between the amines and the surface silanols, partial cleavage of aminosilane siloxy linkages to the oxide surface, and liberation of residual bound water. The additional hydroxyls on the surface may help stabilize chemisorbed CO<sub>2</sub> in the form of carbamic acid, leading to more efficient amine utilization (Fig. S3, ESI†) compared to CO<sub>2</sub> binding as carbamate/ammonium ion pairs.<sup>23</sup> Additionally, <sup>1</sup>H–<sup>29</sup>Si cross-polarization solid-state nuclear magnetic resonance (NMR) spectroscopy shows a slight condensation of the silica surface after thermal treatment at 250 °C (Fig. S10, ESI†), indicating that thermal treatment did not yield significant covalent rearrangement of surface-grafted aminosilanes.

Next, we used TGA-MS to assess the species evolved during elevated thermal treatments. During the 12-hour temperature holds at 200–300 °C, the sorbents did not release enough off-gas products relative to the continuous gas flow through the TGA to generate meaningful MS signals above baseline noise. Because of this analytical limitation, samples were heated to 900 °C at 10 °C min<sup>−1</sup> to increase the volatile species generation rate (Fig. 3a) and probe when degradation occurs in an N<sub>2</sub> atmosphere. Some temperature mismatch with species evolution is expected between these rapidly heated samples and the isothermally treated samples held for 12 hours.

During the 1 hour 100 °C degas step before the temperature ramp, H<sub>2</sub>O (*m/z* = 17, 18) and CO<sub>2</sub> (*m/z* = 44) desorption occurred rapidly, typical of sorbents exposed to ambient air prior to TGA measurement. For all thermal treatments, a similar initial degas step was performed prior to the ramp and hold at the elevated temperature to reduce the possibility

of CO<sub>2</sub>- or H<sub>2</sub>O-related chemical degradation.<sup>13</sup> Once the temperature rose, additional H<sub>2</sub>O was released. This strongly bound water is typical of silica-based materials. Any unreacted methoxy functionalities left from grafting may also further condense and form additional siloxy connections to the silica surface or to other silanes, which also evolves water. Beginning at ~400 °C in Fig. 3a, NH<sub>3</sub> (*m/z* = 16, 17) was produced from amine degradation. Another *m/z* = 44 peak is evolved as well but is more likely associated with an aminosilane degradation fragment rather than CO<sub>2</sub>.

Cyclic adsorption studies were conducted at 250 °C for the high loading ethyl diamine grafted SBA-15 to understand the ultimate utility of the thermal treatments. Fig. 3b–d displays the CO<sub>2</sub> capacity and mass change over multiple cycles in comparison to a control sample only exposed to a 100 °C degas temperature. The control sample exhibited minor fluctuations in the CO<sub>2</sub> capacity (<5%) and mass (<1%), indicating stable performance over multiple cycles. The 250 °C treated sample increased capacity nearly 20% after the first thermal treatment, followed by slowly diminishing improvement until the second thermal treatment step sharply increased the capacity once again. The sample mass decreased with each thermal treatment (cycles 2 and 6), as expected from the elemental analysis and TGA data, yet increased slightly over cycles 3–5. The small yet consistent mass increase over cycles 3–5 could be from water sorption on the silica when the samples were briefly exposed to ambient conditions in between each cycle. The second thermal treatment before cycle 6 is nearly able to replicate the CO<sub>2</sub> capacity seen in cycle 1 yet is slightly lower likely due to amine degradation from the elevated temperature exposure.

Finally, we investigated several other factors that may influence the effectiveness of these thermal treatments. For most of the experiments, the thermal treatment time was fixed at 12 hours. We varied the treatment time from 1 minute to 12 hours for a high loading ethyl diamine grafted SBA-15 exposed to 200 °C (Fig. S4, ESI†). All exposure times yielded an improved CO<sub>2</sub> adsorption capacity compared to the untreated sample, with the greatest increase achieved after 30 minutes. Therefore, there is an optimal time to achieve improved CO<sub>2</sub> desorption and

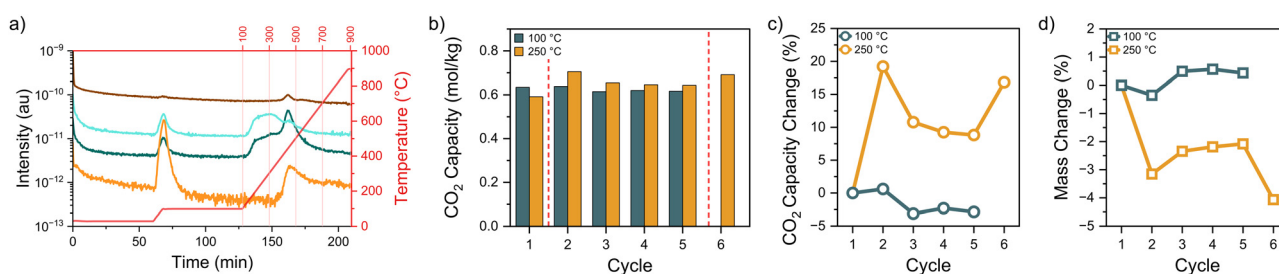


**Fig. 3** (a) MS signals corresponding to CO<sub>2</sub> (*m/z* = 44), H<sub>2</sub>O (*m/z* = 17, 18), and NH<sub>3</sub> (*m/z* = 16, 17) fragments from the off-gas of high loading ethyl diamine grafted SBA-15 heated in N<sub>2</sub>, as well as temperature plotted against TGA experiment time. The temperature profile is shown on the right axis with temperatures repeated on the top axis for clarity. The sample was held at 100 °C for 1 hour before ramping to 900 °C at 10 °C min<sup>−1</sup>. (b) Cyclic CO<sub>2</sub> adsorption results for high loading ethyl diamine grafted SBA-15 thermally treated at either 100 or 250 °C for 1 hour between cycles 1 and 2 (red dashed line). The 250 °C sample was thermally treated a second time between cycles 5 and 6. Where otherwise not indicated, both samples were regenerated at 100 °C. The CO<sub>2</sub> adsorption was measured at 30 °C for 6 hours. (c) The change in CO<sub>2</sub> capacity relative to the first untreated cycle. (d) The change in the degassed sample mass relative to the first untreated cycle.

liberate surface silanols while minimizing amine degradation from high temperatures. We also varied the type of amines (Fig. S5, ESI†) and the grafting supports (Fig. S6, ESI†) to understand the applicability of the thermal treatment. Two additional amines were grafted to SBA-15, 3-aminopropyl trimethoxysilane (designated propyl monoamine) and (6-aminoethyl)aminopropyl trimethoxysilane (designated hexyl diamine), and ethyl diamine was grafted to multiple commercially available oxide supports ( $\text{Al}_2\text{O}_3$ ,  $\text{SiO}_2$ , and  $\text{TiO}_2$ ). Interestingly, the propyl monoamine and hexyl diamine grafted materials showed moderate gains in  $\text{CO}_2$  capacity after 300 °C thermal treatment, as opposed to the sharp decrease for ethyl diamine grafted materials, indicating greater thermal degradation resistance. Additionally, the capacity under a 4%  $\text{CO}_2$  feed (Fig. S7, ESI†) exhibited similar trends, indicating that the change in sorbent performance is not limited to the ultra-dilute  $\text{CO}_2$  concentration of simulated air. Overall, similar trends in the  $\text{CO}_2$  adsorption capacity with thermal treatment temperature were seen across this large array of samples (increased capacity when treated up to 250 °C and decreased capacity after 300 °C for ethyl diamine materials). The changes to the adsorption capacity are neither aminosilane, support, nor gas concentration specific.

In conclusion, we have shown the ability to increase the  $\text{CO}_2$  adsorption capacity for aminosilane-grafted oxide supports *via* elevated temperature thermal treatments. Heating ethyl diamine grafted SBA-15 to 200–250 °C in an inert environment was shown to increase the  $\text{CO}_2$  capacity as much as 21% over conventional degas temperatures of 100 °C (comparison to other materials in Table S6, ESI†). DRIFTS analysis detailed the changes to the sorbent surface species and shift in  $\text{CO}_2$  binding towards carbamic acid species with higher treatment temperatures. TGA-MS analysis of the off gas during heating showed additional water desorption from the silica support at elevated temperatures. The increased  $\text{CO}_2$  capacity from the thermal treatments was maintained over multiple adsorption/desorption cycles and exhibited a similar effect with multiple grafted amine types and support oxide materials. Together, these results suggest that elevated thermal treatments result in improved  $\text{CO}_2$  capacity through the high temperature freeing additional oxide support surface silanols that may in turn help favor more amine efficient  $\text{CO}_2$  binding as carbamic acid. However, prolonged treatment times and higher temperatures increase the degree of amine degradation and affects the ultimate material lifetime. Our findings are generalizable across multiple types of aminosilanes and oxide support materials, thereby offering new insights into the  $\text{CO}_2$  adsorption behavior of grafted amine solid sorbents.

MLJ, NCE, and SHP conceptualized the project. SHP acquired the funding and supervised the project with MMY. MLJ and NCE performed the sorbent characterization experiments. MJR conducted the DRIFTS experiments. EHS synthesized the SBA-15. MATM conducted the solid-state NMR experiments. MLJ wrote the original draft and all authors edited the manuscript.

This work was supported by the U.S. Department of Energy (DOE) Office of Fossil Energy and Carbon Management under

grant FWP-FEW0277. This work was performed under the auspices of the U.S. Department of Energy by Lawrence Livermore National Laboratory under Contract DE-AC52-07NA27344 and was authored in part by the National Renewable Energy Laboratory, managed and operated by Alliance for Sustainable Energy, LLC, for the U.S. DOE under contract no. DE-AC36-08GO28308.

## Data availability

The data supporting this article have been included as part of the ESI.†

## Conflicts of interest

There are no conflicts to declare.

## Notes and references

- M. Bui, C. S. Adjiman, A. Bardow, E. J. Anthony, A. Boston, S. Brown, P. S. Fennell, S. Fuss, A. Galindo, L. A. Hackett, J. P. Hallett, H. J. Herzog, G. Jackson, J. Kemper, S. Krevor, G. C. Maitland, M. Matuszewski, I. S. Metcalfe, C. Petit, G. Puxty, J. Reimer, D. M. Reiner, E. S. Rubin, S. A. Scott, N. Shah, B. Smit, J. P. M. Trusler, P. Webley, J. Wilcox and N. Mac Dowell, *Energy Environ. Sci.*, 2018, **11**, 1062.
- I. P. O. C. Change, *Climate Change 2023: Synthesis Report*, Geneva, Switzerland, 2023.
- L. Küng, S. Aeschlimann, C. Charalambous, F. McIlwaine, J. Young, N. Shannon, K. Strassel, C. N. Maesano, R. Kahsar, D. Pike, M. van der Spek and S. Garcia, *Energy Environ. Sci.*, 2023, **16**, 4280.
- M. Sendi, M. Bui, N. Mac Dowell and P. Fennell, *One Earth*, 2022, **5**, 1153.
- J. Young, N. McQueen, C. Charalambous, S. Foteinis, O. Hawrot, M. Ojeda, H. Pilorgé, J. Andresen, P. Psarras, P. Renforth, S. Garcia and M. van der Spek, *One Earth*, 2023, **6**, 899.
- N. McQueen, K. V. Gomes, C. McCormick, K. Blumanthal, M. Pisciotto and J. Wilcox, *Prog. Energy*, 2021, **3**, 032001.
- M. Erans, E. S. Sanz-Pérez, D. P. Hanak, Z. Clulow, D. M. Reiner and G. A. Mutch, *Energy Environ. Sci.*, 2022, **15**, 1360.
- F. H. Kong, G. Rim, M. Song, C. Rosu, P. Priyadarshini, R. P. Lively, M. J. Realff and C. W. Jones, *Korean J. Chem. Eng.*, 2022, **39**, 1.
- X. Wu, R. Krishnamoorti and P. Bollini, *Annu. Rev. Chem. Biomol.*, 2022, **13**, 279.
- P. A. Saenz Cavazos, E. Hunter-Sellers, P. Iacomini, S. R. McIntyre, D. Danaci and D. R. Williams, *Front. Energy Res.*, 2023, **11**, 1167043.
- J. F. Wiegner, A. Grimm, L. Weimann and M. Gazzani, *Ind. Eng. Chem. Res.*, 2022, **61**, 12649.
- M. J. Lashaki, S. Khiavi and A. Sayari, *Chem. Soc. Rev.*, 2019, **48**, 3320.
- S. A. Didas, R. S. Zhu, N. A. Brunelli, D. S. Sholl and C. W. Jones, *J. Phys. Chem. C*, 2014, **118**, 12302.
- J. Young, E. García-Díez, S. Garcia and M. van der Spek, *Energy Environ. Sci.*, 2021, **14**, 5377.
- A. Heydari-Gorji and A. Sayari, *Ind. Eng. Chem. Res.*, 2012, **51**, 6887.
- I. Nezam, J. Xie, K. W. Golub, J. Carneiro, K. Olsen, E. W. Ping, C. W. Jones and M. A. Sakwa-Novak, *ACS Sustainable Chem. Eng.*, 2021, **9**, 8477.
- M. A. Alkhabbaz, P. Bollini, G. S. Foo, C. Sievers and C. W. Jones, *J. Am. Chem. Soc.*, 2014, **136**, 13170.
- C.-J. Yoo, L.-C. Lee and C. W. Jones, *Langmuir*, 2015, **31**, 13350.
- Y. Meng, T. Ju, F. Meng, S. Han, M. Song and J. Jiang, *ACS Appl. Mater. Interfaces*, 2021, **13**, 54018.
- M. Mureseanu, A. Reiss, I. Stefanescu, E. David, V. Parvulescu, G. Renard and V. Hulea, *Chemosphere*, 2008, **73**, 1499.
- G. Calleja, R. Sanz, A. Arencibia and E. S. Sanz-Pérez, *Top. Catal.*, 2011, **54**, 135.
- R. A. Khatri, S. S. C. Chuang, Y. Soong and M. Gray, *Ind. Eng. Chem. Res.*, 2005, **44**, 3702.
- G. S. Foo, J. J. Lee, C. H. Chen, S. E. Hayes, C. Sievers and C. W. Jones, *ChemSusChem*, 2017, **10**, 266.
- S. A. Didas, M. A. Sakwa-Novak, G. S. Foo, C. Sievers and C. W. Jones, *J. Phys. Chem. Lett.*, 2014, **5**, 4194.
- V. Dugas and Y. Chevalier, *J. Colloid Interface Sci.*, 2003, **264**, 354.

